Flexible, Broadband, Super-Reflective Infrared Reflector based on Cholesteric Liquid Crystal Polymer

Amid Ranjkesh, Yeongyu Choi, Jae-Won Huh, Seung-Won Oh, Tae-Hoon Yoon*

Department of Electronics Engineering, Pusan National University, Busan 46241, Republic of Korea

Corresponding Author

*Tae-Hoon Yoon: thyoon@pusan.ac.kr, TEL: +82-51-510-2379, Fax: +82-51-515-5190

KEYWORDS: liquid crystal; cholesteric liquid crystal polymer; flexible application; IR reflector

ABSTRACT.

Cooling indoor spaces in hot weather conditions requires a significant amount of energy. To reduce energy consumption, light control of windows and facades in buildings is a great way. In this study, we propose a facile method to fabricate a flexible cholesteric liquid crystal (CLC) polymer reflector that can control the reflection of infrared (IR) light selectively without interfering with visible light. To this end, we fabricated a flexible super-wideband IR reflector using right- and left-handed chiral reactive mesogens. The fabricated IR reflector exhibited several desirable properties, including thinness, high mechanical stability and flexibility, strong durability, solvent- and acid resistance, high transparency, and low haze in visible light. The fabricated IR reflector was observed to reduce the indoor temperature by 6 °C compared to the outside temperature. This proves that, by insulating the incident heat, the proposed IR reflector can be utilized to maintain low indoor temperatures in working and living spaces. The flexible and super-reflective CLC film reported in this study is expected to be a promising candidate in several applications, including anti-IR devices, energy-saving windows for cars, and facades of modern buildings.

1. INTRODUCTION

Cholesteric liquid crystals (CLCs) exhibit the characteristic properties of wavelength tuning and polarization-selective reflection.[1–8] CLCs exhibit pitch-selective reflection of the incident light, reflecting wavelengths between $\lambda_{min} = pn_o$ and $\lambda_{max} = pn_e$, where p denotes the pitch of the CLC, and n_o and n_e denote the ordinary and extraordinary refractive indices, respectively. It is known that the reflection bandwidth ($\Delta\lambda = \lambda_{max} - \lambda_{min}$) of CLCs is associated with the birefringence (Δn =

$n_e - n_o$) and pitch p by the relation $\Delta\lambda = p\Delta n$.[9–13] Generally, the maximum reflectance of unpolarized light in CLCs does not exceed 50% because circularly polarized light of the same chirality can be reflected within this reflection band. However, the reflection of both right and left circularly polarized light is observed in nature, particularly in several biological structures and the golden scarab beetle.[14,15]

A reflectance greater than 50% corresponding to a specified wavelength is desirable in several applications that utilize unpolarized radiation. For example, as more than 45% of the total solar energy falls within the infrared (IR) spectrum,[5] reflection of IR light by windows in buildings helps to reduce the energy which is required to cool indoor spaces. Interestingly, if windows accompanied by the reduction of energy on cooling systems could simultaneously control the transparency of the visible light, this kind of windows could be so demanding. Indeed, high transmittance in the visible region can provide indoor lighting, thereby further reducing electricity consumption. In particular, super-reflective or hyper-reflective IR films, which reflect IR light without absorbing any of its energy or affecting the transmission of visible light, are the most effective in reducing the energy consumption of cooling systems.[3–6,14]

Several approaches are commonly used to fabricate super-reflective or hyper-reflective CLC films.[3,16,17] For example, the washout-refill-assembly approach functions by refilling polymers into assembled CLC films.[18] Alternatively, a stack of two individual CLC cells with the opposite handedness can be used.[19] A half-wave plate can also be used between two separate CLC thin films with the same handedness.[20] However, the approaches mentioned above suffer from several issues, including increased insertion loss owing to a large number of interfaces, low stability, high weight, complicated design and fabrication methods, and waste of expensive

materials during the fabrication process of the washout-refill-assembly approach. Moreover, most of the fabricated CLC films exhibit tunable properties and respond to external stimuli, such as mechanical stress, temperature, chemical materials, and electric fields.[21–25] Although this may be useful in some cases, susceptibility to external stimuli can be a disadvantage in several applications. Except for susceptibility to external stimuli, most reported CLC films cannot block the solar IR radiation because they are designed for the visible region,[26–29].

A few previous attempts to fabricate IR reflectors[30,31] have revealed that a single temperature-independent device with high mechanical stability, adequate resistance to chemical attacks, broadband reflectivity, flexibility, and heat insulation would be advantageous for various applications. However, a single device with all the properties mentioned above has not yet been reported in the literature. In particular, the fabrication of a temperature-independent, flexible, broadband, and super-reflective IR reflector without interfering with the visible spectrum of light is considered an essential demand in modern building's indoor spaces and cars. Furthermore, an inexpensive method that uses a minimal number of layers to design the required shapes with high flexibility, and maintains the transparency of the visible light would be preferable.

To address this demand, in this study, we report the fabrication of a flexible, broadband, and hyper-reflective IR reflector comprising only two polymer layers. The proposed IR reflector was verified to successfully reflect more than 90% of the incoming IR light corresponding to the range of wavelengths between 800 nm and 1200 nm. Furthermore, owing to the reduced number of layers, the proposed IR reflector exhibited complete transparency and low haze for the visible spectrum of light. Previous reports have established that solar IR radiation lies in wavelengths between 700 nm and 1 mm.[3–5] Therefore, we focused on reflecting this relatively small span of

wavelengths. Experimental results demonstrated the applicability of the proposed IR reflector over a wide temperature range because of the permanent solid helical structure and temperature-independent pitch length of the polymer network in the CLC film. Furthermore, the proposed film enabled precise control of the reflection band location via the experimental procedure. Such an IR film with a freestanding character engenders new approaches to various flexible applications. It provides significant freedom to the design of the required shapes while ensuring a standard of performance. Therefore, the fabrication of the flexible, broadband, and super-reflective CLC film with no temperature dependence and high stability reported in this study can be considered a significant achievement.

2. EXPRIMENTAL SECTION

2.1 MATERIALS

For the proposed fabrication process, we used a left-handed chiral reactive mesogen (RM) (HCM-006, HCCH, China) with a helical twisting power (HTP) of 57 μm^{-1}, a right-handed chiral RM (LC-756, HTP = 76 μm^{-1}, BASF), monoacrylate monomer 4-Methoxybenzoic acid 4-(6-acryloyloxyhexyoxy) phenyl ester (ST03866, SYNTHON), diacrylate monomer RM-257 (BASF), an ultraviolet (UV) light absorber (2-hydroxyphenyl-benzophenones, Chimassorb 81, BASF), and a photoinitiator (Irgacure 651, BASF). All the materials mentioned above were used without any further purification. The chemical structures of these materials are presented in Figure 1. Depending on the HTP of the chiral RMs, two separate CLC mixtures were prepared to fabricate IR reflectors—a left-handed CLC mixture including RM-257/ST03866/HCM-006/Chimassorb 81/Irgacure-651 (weight ratio 73/23/3/1/1) and a right-handed CLC mixture containing RM-257/ST03866/LC-756/Chimassorb 81/Irgacure-651 (weight ratio 73/22/4/1/1). To induce the UV

intensity gradient along the cross-section of the film, a UV light absorber (Chimassorb 81, BASF) was added to the CLC mixture. The UV light absorber also stabilizes the polymer film properly, as reported in. [9,11]

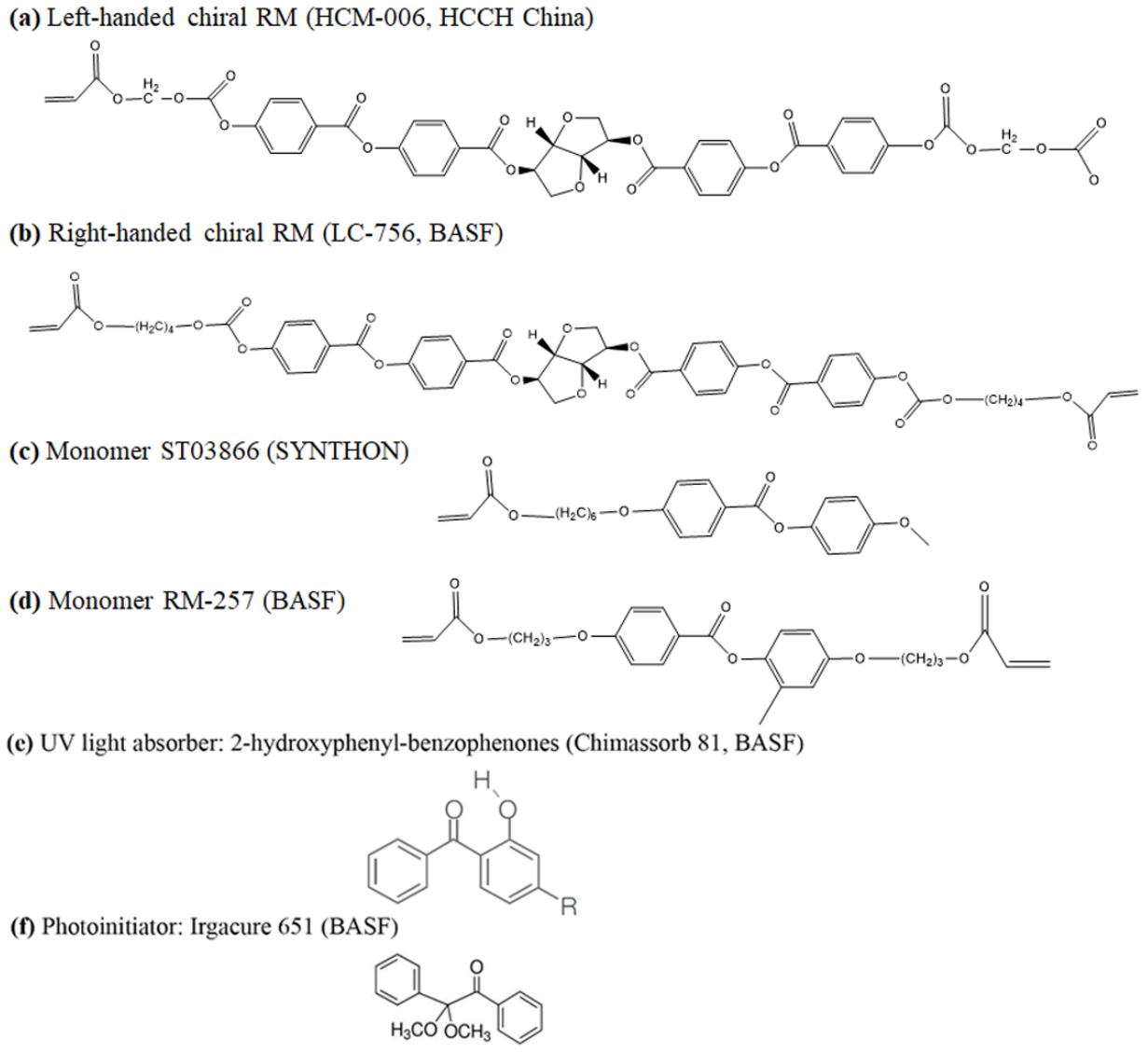

Figure. 1 Materials used in this study and their chemical structures.

2.2 SAMPLE PREPERATION AND EXPRIMENTAL PROCEDURE

A polyethylene terephthalate (PET) film was cleaned and spin-coated with a planar polyimide alignment layer (SE6514, Nissan) and subsequently baked at 180 °C for 30 min. A rubbing process was utilized to ensure the planar alignment of the deposited layer. Following this, a doctor blade coating process was applied to the film to coat the mixture at an appropriate speed. The film was then exposed to UV light (Newport, Co., LTD) emitted from a mercury arc lamp (Osram HBO 103 W/2) with an intensity of 0.1 mW/cm^2 under a nitrogen atmosphere for 30 min at 50 °C. Finally, the samples were post-cured for 10 min under high UV flood exposure with an intensity of 20 mW/cm^2.

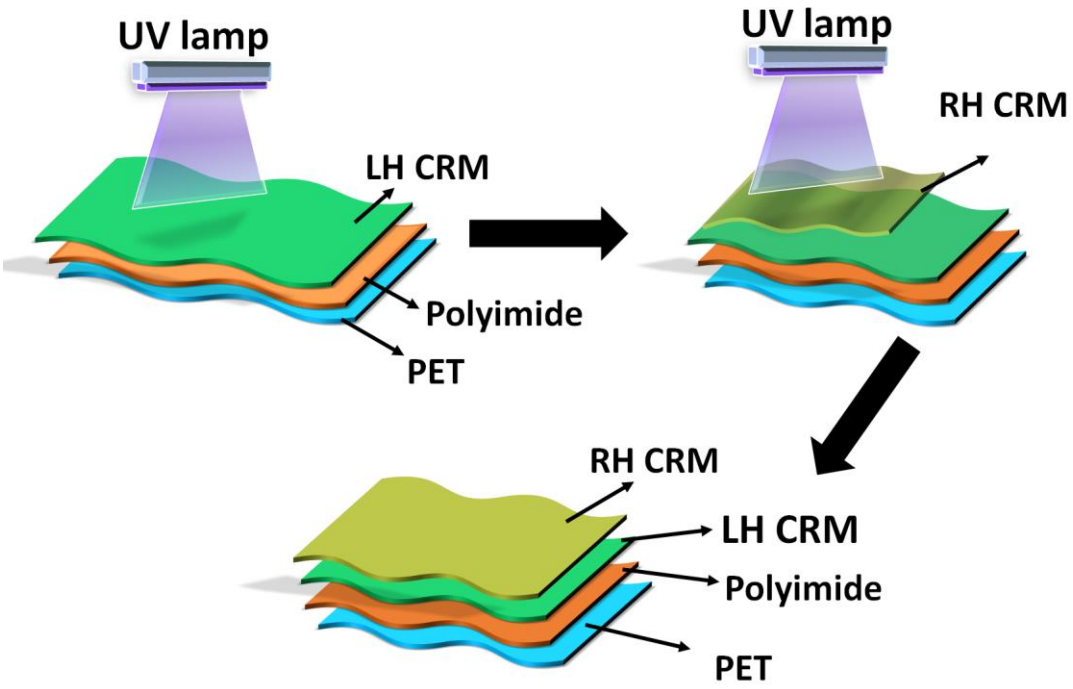

Figure.2 Schematics illustration of the fabrication of the flexible, broadband, super-reflective IR reflector film using sequential layer-by-layer of right- and left-handed chiral RMs as superimposed on each other along with a photo-polymerization process.

To induce nearly 100% reflection of unpolarized infrared light with the fabricated samples, two different broadband CLC films with opposite-handed reflection were directly coated on PET to form a superimposed, super-reflective, and broadband polymer bilayer. The experimental process is illustrated in Figure 2. The transmission spectra were measured using a spectrometer (Flame-NIR Spectrometer, Ocean Optics), and the surface texture of the film was investigated using a three-dimensional (3D) optical surface profiler (Nanosurface Profiler NV-E1000, Nano System Co., Ltd.).

3. RESULT AND DISCUISSION

The fabricated right-handed CLC mixture was designed to realize a reflection peak centered at 1090 nm before polymerization. After the UV-polymerization, a broadband reflective film with $\Delta\lambda = 274$ nm was obtained. The left-handed polymer film exhibited a reflection band centered at 1095 nm with $\Delta\lambda = 283$ nm after the UV-polymerization. Figure 3 depicts the transmission spectra of the left- and right-handed polymer CLC films before and after exposure to the low-intensity UV light for polymerization followed by the exposure to the high-intensity UV light.

In CLCs, $\Delta\lambda$ is known to be highly dependent on Δn of the LC. Because of the low value of Δn in LCs, their $\Delta\lambda$ values are usually inadequate for reflection of a significant amount of IR light. To broaden the $\Delta\lambda$ value of the fabricated CLC film, a UV light absorber (Chimassorb 81) was used. The UV light absorber absorbs UV radiation and generates a UV-intensity gradient within the film. In other words, absorption of UV light induces a UV-intensity gradient within the CLC mixture upon UV irradiation, which has also been reported in.[27,32,33] Notably, the UV light absorber prevents degradation of the substrate, robustly stabilizes the polymer film, and improves the durability of the polymeric film against external forces.[9, 27] To show the significant effect of

the UV light absorber to broaden the Δλ, we can eliminate the UV light absorber in the fabricated CLC film. Figure S1 reveals that the film fabricated without the UV light absorber exhibits a narrow IR reflection band. Therefore, by comparing Figure S1 with Figure 3, the broadened Δλ can be attributed to the UV light absorber.

Figures 3a and 3b illustrate the broadband reflection of circularly polarized IR light for the left-handed (900–1250 nm) and right-handed (910–1245 nm) CLC films. Both left- and right-handed CLC films appeared transparent in visible light. Their broadband reflection can be attributed to the diacrylate forms of chiral RMs, which induce maximal concentration of chiral RMs at the top sides of the films exposed to UV light. Chiral RMs polymerize faster at the top side of the film than at the bottom because of the high UV intensity in that area. Thus, the diffusion of chiral RMs from the bottom to the top side and the consequent non-uniform distribution creates a pitch gradient along the cross-section of the film.[17,27] Indeed, this pitch gradient is responsible for the observed broadband reflection.

Several factors influence the observed broadband reflection characteristics, including the UV-illumination duration, the difference in reactivity between the chiral RMs, and the viscosity of each CLC mixture. For example, as illustrated in Figure S2, exposure to high-intensity UV light over a short duration (*e.g.*, 5 min) can lead to a narrower reflection band of the CLC films because the RMs move rapidly toward the top side (the side exposed to the UV lamp) by the high UV intensity; thus preventing the formation of a pitch gradient within the film.[34] On the other hand, the opportunity to move to the top side of the film and build the pitch gradient are afforded to the UV light absorber and the RMs when exposed to UV light of low intensity.

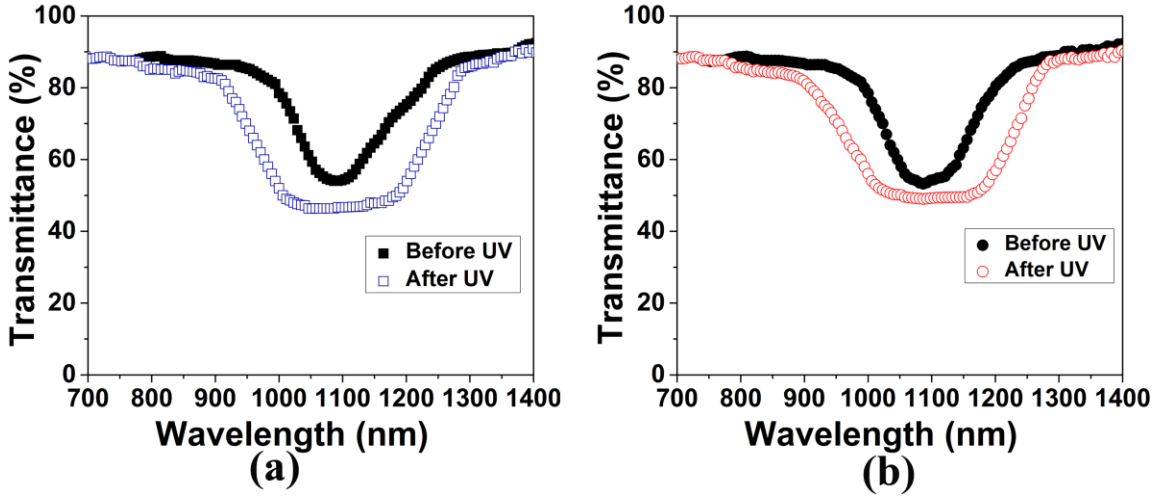

Figure.3 Transmission spectra of CLC polymer film. (a) left-handed and (b) right-handed CLC mixtures before and after a low-intensity UV exposure for polymerization followed by a high-intensity UV exposure.

Figures 4a depicts super-reflective and broadband polymer bilayers, fabricated using right- and left-handed broadband films. Two CLC films with almost the same characteristics, except for their opposite handedness, were used to simplify the method as far as possible. As is evident from Figure 4a, the fabricated film exhibits broadband reflection of unpolarized IR light (~820 to 1320 nm). Thus, the broadband IR reflector is expected to reflect most of the incident IR energy when it is coated on the surface of a window.

To evaluate the optical performance of the fabricated IR reflector after bending the CLC films, its specular transmittance and haze were measured using a haze meter (HM-65W, Murakami Color Research Laboratory). Total transmittance (T_t) is defined to be the sum of specular transmittance (T_s) and diffuse transmittance (T_d).[36] Haze (H) is calculated using $H = Td/Tt$.[37] As is

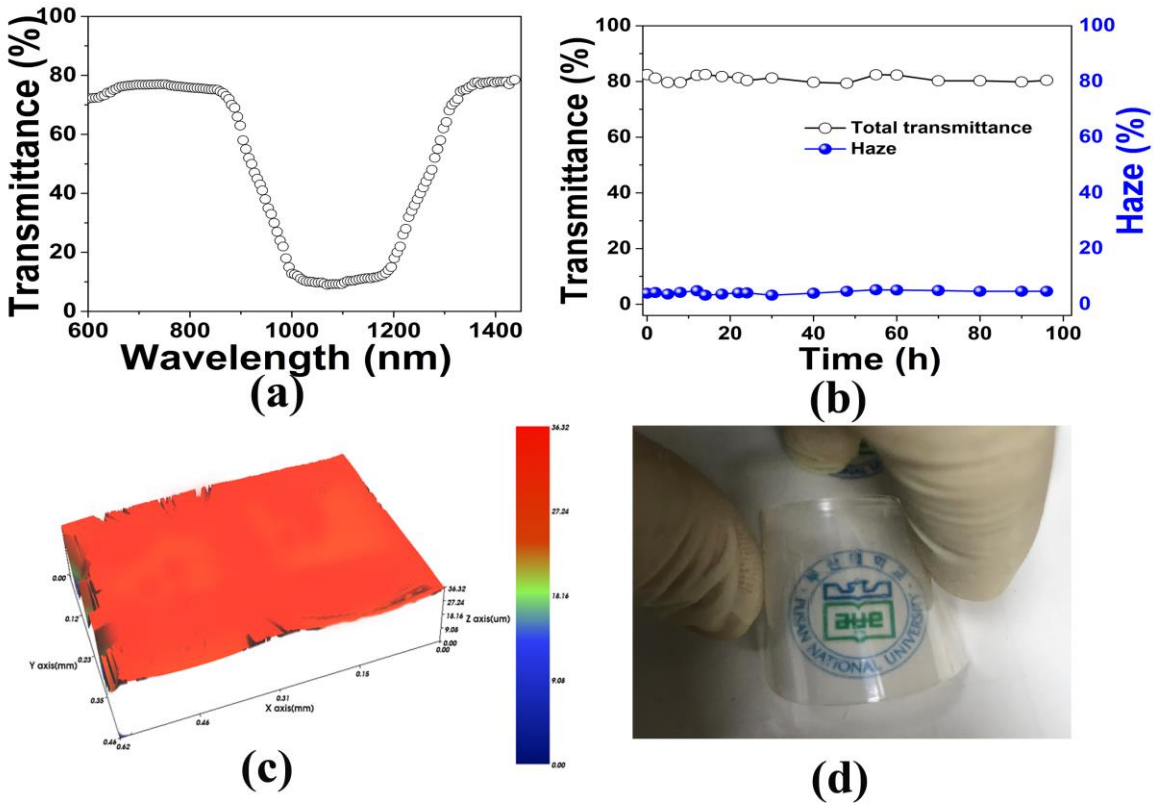

Figure. 4 (a) Transmission spectra of right- and left- handed films superimposed on each other. (b) Total transmittance and haze values of the CLC film. (c) Surface profile of the fabricated film obtained with a 3D optical surface profiler. (d) Photographs of the fabricated CLC polymer films demonstrate high transparency of the films at bending condition.

evident from Figure 4b, the IR reflector does not exhibit significant degradation in optical performance even after being deformed for a long time. Total transmittance and haze of the fabricated IR reflector were 82.7% and 3.3%, respectively. These values confirm that the fabricated IR reflector is transparent to visible light when used to coat the window's surface. It is to be noted that the fabricated IR reflector is very compact and thin. The thickness of the film was

measured to be only 36.4 μm using a 3D optical surface profiler, as shown in Figure 4c. Figure 4d depicts an actual photograph of the fabricated CLC polymer film, exhibiting high transparency and low haze even under deformation.

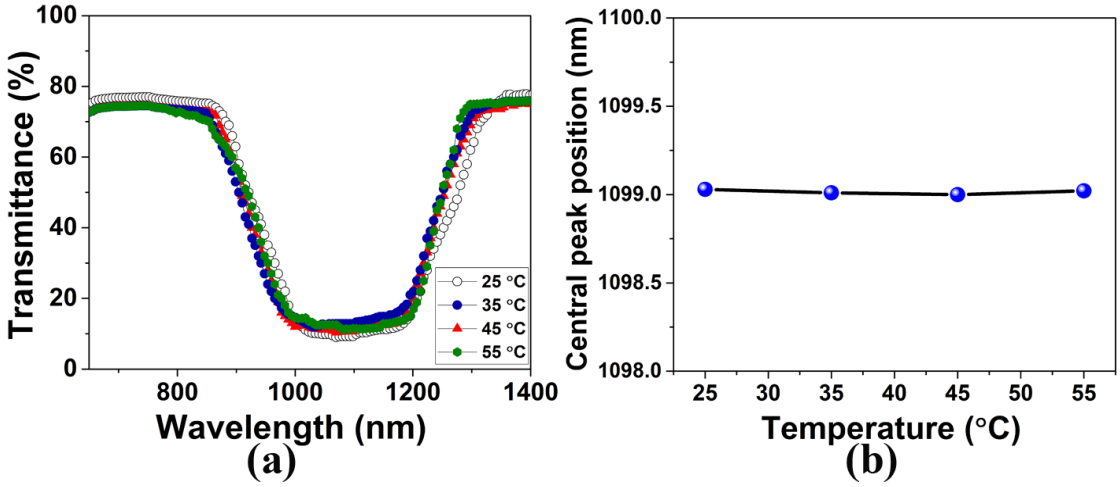

Figure. 5 (a) Temperature-dependent transmission spectra of the CLC film upon varying the temperature from 25 to 55 ºC. (b) Center wavelengths of the CLC films at different temperatures.

It is interesting to note that the proposed IR reflector is temperature-independent owing to the excellent stability of the Bragg reflection band at elevated temperatures. To confirm this characteristic, transmission measurements were performed at temperatures ranging between 20°C and 55°C. The effect of temperature on the films was evaluated using a Mettler FP82 hot stage controlled by a Mettler FP90. The central wavelengths of the reflection spectra were observed to remain almost unchanged with a negligible shift. Thus, the fabricated IR film exhibits approximately the same reflection band over the temperature range, as depicted in Figures 5a and

5b. This establishes the viability of applying the proposed IR reflectors under most global weather conditions without affecting the performance of the CLC polymer film significantly. It should be noted that both the right- and left-handed polymer films exhibited high stability of the reflection band at elevated temperatures—the spectra were almost the same over temperatures ranging between 25 °C and 70 °C (Figure S3 in ESI†). Thus, the fabricated temperature-independent LC polymer films are expected to be suitable for most populated terrestrial places.

Although the fabricated super-high reflective CLC films are promising for potential applications, to check the appropriateness of the IR film in various applications, several other parameters such as mechanical stability, sensitivity to the external environment, and the durability of the film should be tested. To this end, we performed additional tests on IR polymer film to evaluate their flexible strength, resistance to chemical attacks, and durability. To measure mechanical stability, several types of mechanical deformation were tested, including bending, folding, twisting, radius-of-curvature limit, as depicted in Figure 6. The fabricated IR film exhibited excellent mechanical stability and no flexural resistance during and after repetitive mechanical deformation (*e.g.*, bending to various angles, folding, and rolling).

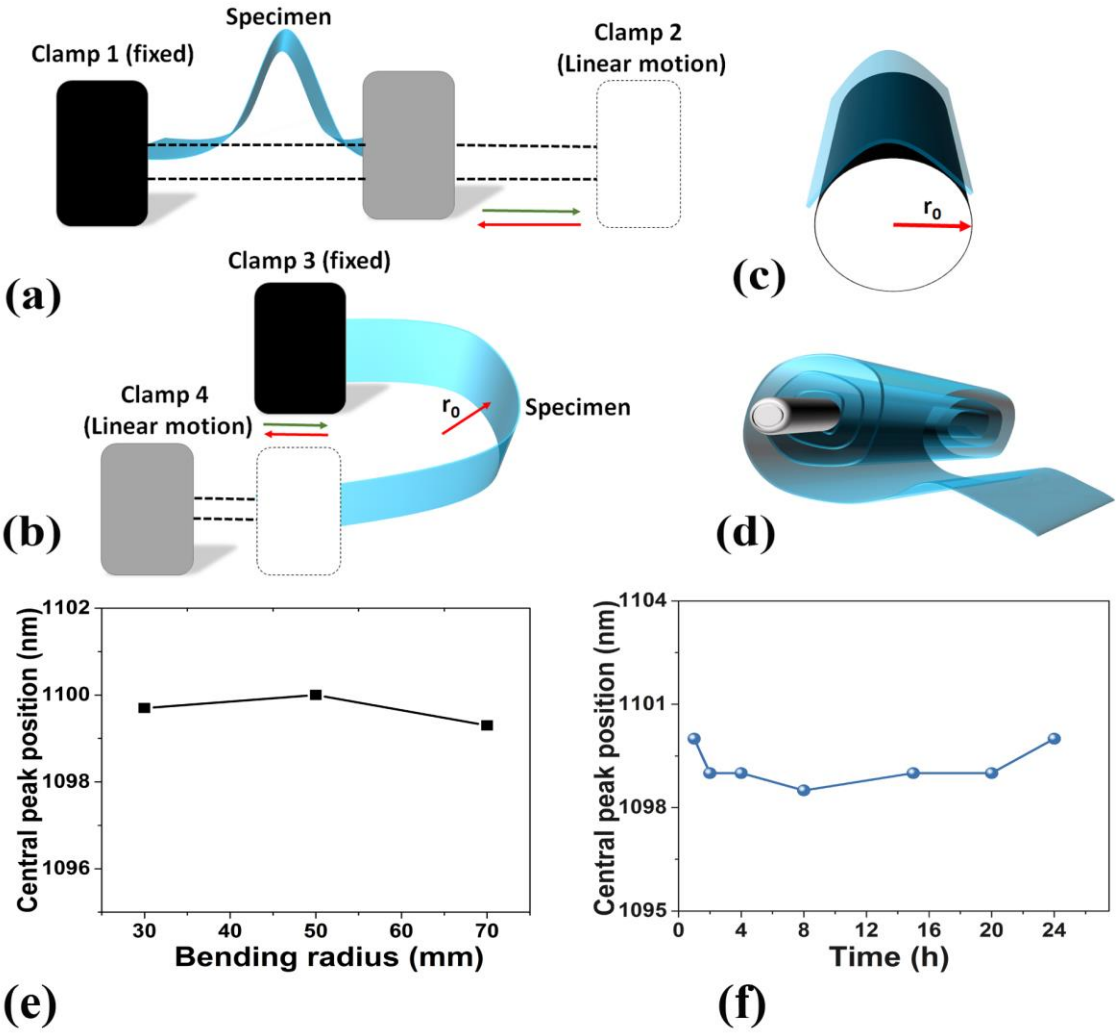

Figure. 6 Schematics of various deformation modes for the CLC film: (a) linear bending mode; (b) sliding mode; (c) radius-of-curvature limit test on a cylinder with a certain bending radius; and (d) rolling mode. Center wavelengths of the CLC films for (e) different bending radii of 30, 50, and 70 mm, bent for 24 h at room temperature (25 °C); and as (d) a function of time to measure the lifetime of the CLC film for 24 h at room temperature (25 °C).

To perform the radius-of-curvature limit test, the fabricated films were wrapped onto three cylindrical holders with different radii (*i.e.,* 30, 50, and 70 mm) at room temperature (25 °C) for 24 h. Then, they were detached from the cylinders, and their transmission characteristics were analyzed. The fabricated IR films were observed to return to their original state without any performance degradation (*e.g.*, cracks or wrinkles) even after repeated bending fatigue tests. As illustrated in Figure 6e, the peak reflection wavelength by the fabricated CLC film remained almost the same after bending. As shown in Figure 6e, no significant performance degradation was observed after the bending of the film. Finally, to evaluate the expected lifetime of the fabricated IR film, the center wavelengths of the peak reflection by the films were measured as a function of time, as depicted in Figure 6f. Based on our results, it can be concluded that the fabricated IR film exhibits excellent mechanical stability.

To verify the chemical stability of the fabricated CLC IR films, tests were conducted using two types of chemicals—organic solvents and acids. As acid rain is known to degrade facades of buildings and turn windowpanes misty, an acid-resistance test would be an essential analysis for the fabricated IR film. In the experiment, organic solvents were first dropped onto the surface of the film, and then the film was drowned in the organic solvents. To evaluate the acid resistance of the fabricated IR film, it was covered with Norland Optical Adhesive (NOA 68). Figure 7 presents actual photographs of the IR film during the aforementioned experiments involving different solvents. The results established the stability of the fabricated IR films against chemical attacks using organic solvents and acids, and no performance degradation was observed. Movies S1 and S2 depict the resistances of the IR films against various chemical solvents and acids, respectively. To test the acid resistance of the polymer IR film, we used two different acids—acetic acid as a weak acid and hydrochloric acid as a strong acid. To demonstrate the chemical reaction of acids

to substrates and materials, we tested the chemical reaction of the two acids to the salt as a reference. As shown in movie S2, the salt appropriately dissolved in both acids. As evidenced by the movie S2, for both acids, the IR films were observed to be stable, and the transparency of the films was not diminished.

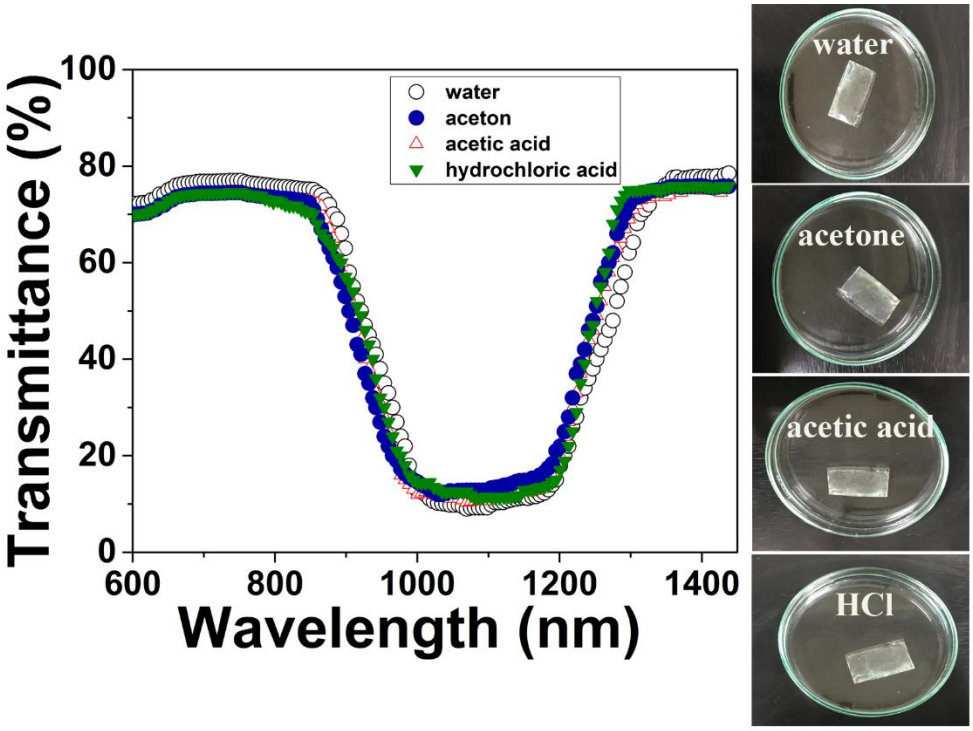

Figure. 7 Transmission spectra of the CLC film for different organic solvents (i.e., water and acetone) and acids (acetic acid as a weak acid and hydrochloric acid (HCl) as a strong acid) to demonstrate the chemical stability of the film.

Next, the durability of polymer IR film was evaluated. To this end, a tape peeling adhesion test was conducted to estimate the degree of adhesion of the CLC polymer to the PET substrate with CLC coatings on the surfaces. Based on the results, the rating was assigned by “Standard Test

Methods for Measuring Adhesion by Tape Test" based on the ASTM D3359 standard.[35]A tape was manually attached to the IR CLC film and then rapidly removed. The test was repeated as we varied peel angles between 0° and 90° with the same tape application pressure, as depicted in Figure 8. The peel adhesion test revealed excellent robustness without any degradation irrespective of the peel angle within the indicated range. No debris was observed on the tested tape side after peeling off the tape, and the IR film surface was also decontaminated. As a result, the fabricated IR films were assigned a rating of 4 A level in terms of the adhesion strength based on the ASTM D3359 standard.[35] The movie S3 depicts the performance of the fabricated IR reflective film under the peel adhesion test. It was evident that the polymer film was firmly attached to the PET, and no degradation was observed after peeling off the tape.

It is well known that, with an increase in the incident angle, the Bragg reflection band in CLCs shifts to a shorter wavelength,[39,40] thereby exhibiting a blue shift at oblique incidence. In our case as well, the change in the effective helical pitches of the CLC layers results in a shift of the center wavelength of the Bragg reflection. For normal incidence, the center wavelength is given by $\lambda_o = np_o$, where p_o denotes the CLC pitch length, and n denotes the average refractive index defined by $n = (n_e + n_o)/2$, where n_o and n_e denote the ordinary and extraordinary refractive indices, respectively. By contrast, for an oblique incidence angle Θ, the center wavelength of the Bragg reflection is given by $\lambda = np_o \cos\Theta$ within the CLC, where Θ is related to the incident angle in air θ, by the Snell's law—$\Theta = \sin^{-1}(1/n\sin\theta)$.[39]

Figure 9a presents the reflectance of IR light of the IR CLC film as a function of the viewing angle, and Figure S4 shows the transmission spectra at a different viewing angle from 0º

to 60º for the CLC film. As evident from Figures 9a and S4, blue-shift tuning reflection was observed upon altering the viewing angle from 0º to 60º. This indicates that the fabricated IR CLC

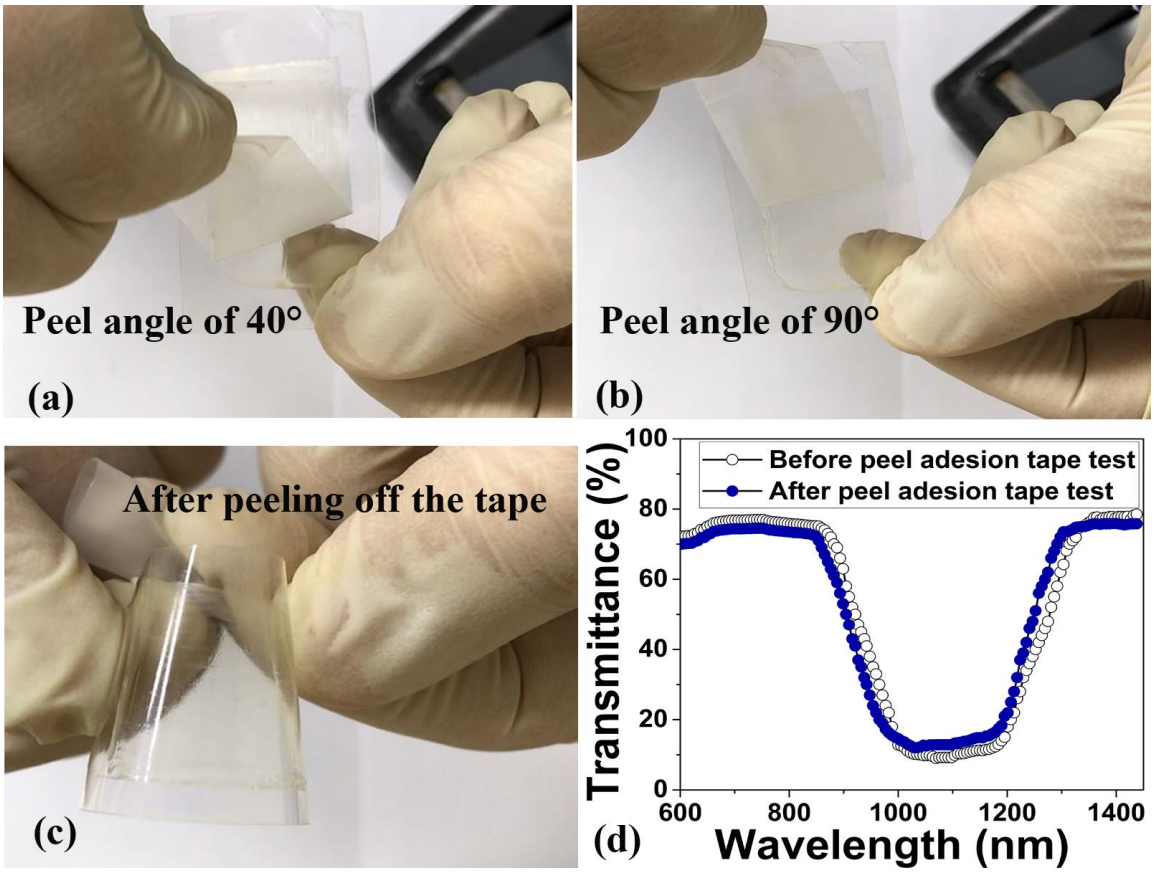

Figure. 8 Photographs of the peeling-off test for the CLC film. First, press the adhesive tape firmly to the surface of the film, then the tape is peeled off at an angles of (a) 40º and (b) 90º. (c) The Photographs of the fabricated CLC film after peeling off the adhesive tape without any performance degradation. (d) Transmission spectra of the CLC film before and after the peel adhesion test.

film reflects a greater amount of heat over a broader range of the incidence angle. Figure 9b verifies this conclusion by showing that larger angles of incidence correspond to lower temperatures. Thus, the proposed IR reflector exhibits better performance at oblique incidence. As the range of the incidence angle of the midday sun is broader in summer than in winter in the northern hemisphere, as depicted in Figure 9c, the proposed IR film reflects a greater amount of sunlight in summer.

To analyze the actual thermal control properties of the fabricated IR reflectors more comprehensively, a test house at size 3 cm × 3 cm × 3 cm was built with the proposed IR reflector film. The house model did not possess any solar shading system. A thermocouple thermometer was placed inside the house to monitor the indoor temperature collected once every 5 min for 60 min. Then, the test house was placed under direct sunlight, which penetrated the IR reflector-laced window and affected the indoor temperature of the house. To investigate the effect of the IR reflector on indoor temperature, we fabricated two test houses—a house built with each instant of measurement—the temperature inside the house built with the IR house was observed to be lower than that in the house built with PET. In the PET house, the indoor temperature attained a maximum of approximately 60.4 °C. On the other hand, the indoor temperature of the house built with the proposed IR reflector reached a maximum of only 39.6 °C. These results indicate that the indoor temperature can be effectively controlled by selectively blocking or transmitting near-IR (NIR) light. The proposed IR reflector appropriately reflects the IR light and successfully prevents the house from heating up due to exposure to sunlight.

Figure 9d demonstrates that the temperature in the house built with the IR reflector films was lower than that in the house built with conventional PET. The experiment was conducted in the early spring when solar emission is not very intense. A much higher temperature difference

can be expected if a similar experiment is performed during summer. The heat insulation test establishes the viability of using the polymer IR reflector proposed in this study to design highly efficient energy-saving windows and facades in hot weather conditions.

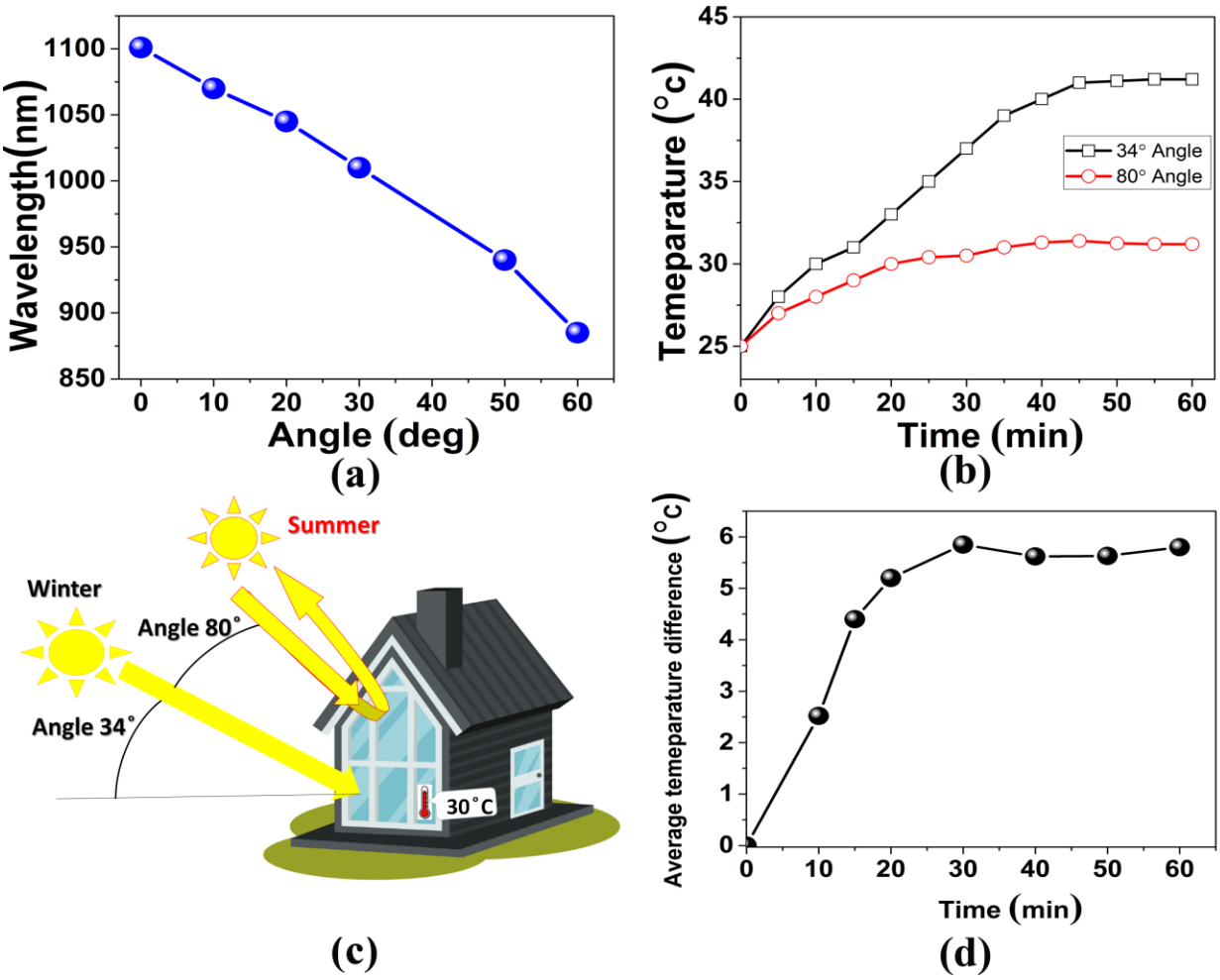

Figure. 9 (a) Transmission spectra at a different viewing angle from 0º to 60º for the CLC film at room temperature 25 ºC. (b) Temperature measurement with time of the thermal insulation heat miniature house covered with a CLC reflector. (c) Schematic of the range of midday sun angles at 33° north latitude. (d) The average temperature difference for the fabricated CLC reflector when the window faces the sun rays for 0 to 60 min.

It should be emphasized that the proposed IR reflector exhibited high transparency for visible light of natural color. However, it reflected a significant proportion of the incident IR light without any effect on the visible portion of the solar spectrum. This characteristic is essential for the construction of windows contrasts with a low-solar-gain-type window where a decrease of the temperature accompanies the reduction of the view and unusual color change. The proposed IR reflector film is expected to be practically beneficial in designing next-generation windows to reduce the energy consumption required by cooling systems without disturbing the spectrum of visible light.

4. CONCLUSION

In this study, we introduced a facile method to fabricate CLC polymer reflectors capable of selectively controlling IR reflection. To this end, right- and left-handed chiral RMs were coated on PET without using any intervening alignment layer. The fabricated IR reflector exhibited a super-wide reflection band, sufficient flexibility under mechanical deformation, and high transparency in the visible spectrum of light. Effective control and blocking of light in IR wavelengths could be achieved by appropriately selecting the helix pitch in the CLC networks of chiral RMs. Compared to previously reported IR reflectors, the CLC polymer films proposed in this study exhibited the intrinsic advantages of being compact, super-reflective, broadband, and flexible. The proposed IR reflector was demonstrated to possess maximum freedom to fabricate irregular shapes and exhibit high flexibility, rollability, and mechanical deformation without any detrimental effects on appearance or performance.

The proposed polymer CLC reflector can be used to reflect IR light in buildings, cars, greenhouses, and indoor spaces, enabling the maintenance of comfortable indoor temperatures without the use of cooling devices. This induces a considerable reduction in energy consumption. Moreover, the proposed IR reflector accompanies an effective reflection of solar IR energy with low optical haze, high transparency, and no disturbance to the visible spectrum of light. The reduction in indoor temperature achieved by implementing the IR film was confirmed based on a heat insulation test. We expect the proposed flexible, broadband, and super-reflective IR film to be employed in various large-scale applications and potentially serve as reflectors in energy-saving windows, building facades, and anti-IR devices.

Supporting Information

The Supporting Information is available free charge on the ACS Publications website at DOI:

Transmission spectra of left- and right-handed CLC polymer film by excluding the UV light absorber; Transmission spectra of fabricated polymer CLC film at 5 minute UV light irradiation; Temperature-dependent transmission spectra of right- and left- handed CLC films upon varying the temperature from 25 ºC to 70 ºC; Transmission spectra at a different viewing angle from 0º to 60º for the CLC film at room temperature 25 ºC; Change in the indoor temperature for the sets of houses for conventional PET, and the proposed IR reflector.

ORCID

Amid Ranjkesh: 0000-0002-4411-5606

Tae-Hoon Yoon: 0000-0002-9047-8002

Jae-Won Huh: 0000-0002-4512-2971

Seung-Won Oh: 0000-0001-7596-948X

ACKNOWLEDGMENTS

This work was supported by a National Research Foundation of Korea (NRF) (No. 2020R1A2C1006464).

REFERENCES

(1) Ostwald, P.; Pieranski, P. Nematic and Cholesteric Liquid Crystals. CRC, Boca Raton, 2005.

(2) Bahr, C.; Kitzerow, H. S. Chirality in Liquid Crystals. Springer, Heidelberg, 2001.

(3) Mitov, M. Cholesteric Liquid Crystals with a Broad Light Reflection Band. *Advanced Materials*., **2012**, *24*, 6260–6276.

(4) Mitov, M. Going beyond the reflectance limit of cholesteric liquid crystals. *Nature Materials*, **2006**, *5*, 361–364.

(5) Khandelwal, H.; Loonen, R. C. G. M.; Hensen, J. L. M.; Schenning, A. P. H. J.; Debije, M. G. Application of broadband infrared reflector based on cholesteric liquid crystal polymer bilayer film to windows and its impact on reducing the energy consumption in buildings. *Journal of Materials Chemistry A* **2014**, *2*, 14622-14627.

(6) Kim, J.; Kim, H.; Kim, S.; Choi, S.; Jang, W.; Kim, J.; Lee, J.-H. Broadening the reflection bandwidth of polymer-stabilized cholesteric liquid crystal via a reactive surface coating layer. *Applied Optics* **2017**, *56*, 5731-5735.

(7) Davies, D. J. D.; Vaccaro, A. R.; Morris, S. M.; Herzer, N.; Schenning, A. P. H. J.; Bastiaansen, C. W. M. A Printable Optical Time-Temperature Integrator Based on Shape Memory in a Chiral Nematic Polymer Network. *Advanced Functional Materials* **2013**, *23*, 2723–2727.

(8) Guo, J.; Cao, H.; Wei, J.; Zhang, D.; Liu, F.; Pan, G.; Zhao, D.; He, W.; Yang, H. Polymer stabilized liquid crystal films reflecting both right-and left-circularly polarized light. *Applied Physics Letters* **2008**, *93*, 201901-201903.

(9) Ranjkesh, A.; Yoon, T.-H. Thermal and electrical wavelength tuning of Bragg reflection with ultraviolet light absorbers in polymer-stabilized cholesteric liquid crystals. *Journal of Materials Chemistry C* **2018**, *6*, 12377-12385.

(10) Li, Y.; Liu, Y.; Luo, D. Optical thermal sensor based on cholesteric film refilled with mixture of toluene and ethanol. Optics express. *Optics Express* **2017**, *25*, 26349-26355.

(11) Ranjkesh, A.; Yoon, T.-H. Fabrication of a Single-Substrate Flexible Thermoresponsive Cholesteric Liquid-Crystal Film with Wavelength Tunability. *ACS applied materials & interfaces*, **2019**, *11*, 26314-26322.

(12) Wu, P.-C.; Wu, G.-W.; Timofeev, I. V.; Zyryanov, V. Y.; Lee, W. Electro-thermally tunable reflective colors in a self-organized cholesteric helical superstructure. *Photonics Research* **2018**, *6*, 1094-1100.

(13) Hsiao, Y.-C.; Yang, Z.-H.; Shen, D.; Lee, W. Red, green, and blue reflections enabled in an electrically tunable helical superstructure. *Advanced Optical Materials* **2018**, *6*, 1701128, 5050-5054.

(14) Mitov, M. Cholesteric Liquid Crystals in Living Matter. *Soft Matter* **2017**, *13*, 4176–4209.

(16) Mcdonald, L. T.; Finlayson, E. D.; Wilts, B. D.; Vukusic, P. Circularly Polarized Reflection from the Scarab Beetle Chalcothea Smaragdina: Light Scattering by a Dual Photonic Structure. *Interface Focus* **2017**, *7*, 20160129.

(17) Balamurugan, R.; Liu, J.-H. A review of the fabrication of photonic band gap materials based on cholesteric liquid crystals. *Reactive and Functional Polymers* **2016**, *105*, 9-34.

(18) Kim, D.-Y.; Lee, K. M.; White, T. J.; Jeong, K.-U. Cholesteric liquid crystal paints: in situ photopolymerization of helicoidally stacked multilayer nanostructures for flexible broadband mirrors. *NPG Asia Materials* **2018**, *10*, 1061-1068.

(19) Li, Y.; Liu, Y.J.; Dai, H.T.; Zhang, X.H.; Luo, D.; Sun, X.W. Flexible cholesteric films with super-reflectivity and high stability based on a multi-layer helical structure. *Journal of Materials Chemistry C* **2017**, *5*,10828-10833.

(20) Mcconney, M. E.; Tondiglia, V. P.; Hurtubise, J. M.; Natarajan, L. V.; White, T. J.; Bunning, T. J. Thermally Induced, Multicolored Hyper-Reflective Cholesteric Liquid Crystals. *Advanced Materials* **2011**, *23*, 1453–1457.

(21) Mcconney, M. E.; Tondiglia, V. P.; Hurtubise, J. M.; White, T. J.; Bunning, T. J. Photoinduced Hyper-Reflective Cholesteric Liquid Crystals Enabled via Surface Initiated Photopolymerization. *Chem. Commun.* **2011**, *47*, 505–507.

(22) Lee, C. S.; Kumar, T. A.; Kim, J. H.; Lee, J. H.; Gwag, J. S.; Lee, G.-D.; Lee, S. H. An electrically switchable visible to infra-red dual frequency cholesteric liquid crystal light shutter. *Journal of Materials Chemistry C* **2018**, *6*, 4243-4249.

(23) Mcconney, M. E.; White, T. J.; Tondiglia, V. P.; Natarajan, L. V.; Yang, D.-K.; Bunning, T. J. Dynamic High Contrast Reflective Coloration from Responsive Polymer/Cholesteric Liquid Crystal Architectures. *Soft Matter* **2012**, *8*, 318–323.

(24) Ryabchun, A.; Bobrovsky, A. Cholesteric Liquid Crystal Materials for Tunable Diffractive Optics. *Advanced Optical Materials* **2018**, *6* (15), 1800335.

(25) Nickmans, K.; Heijden, D. A. C. D.; Schenning, A. P. H. J. Photonic Shape Memory Chiral Nematic Polymer Coatings with Changing Surface Topography and Color. *Advanced Optical Materials* **2019**, *7*, 1900592.

(26) Bian, Z.; Li, K.; Huang, W.; Cao, H.; Yang, H.; Zhang, H. Characteristics of Selective Reflection of Chiral Nematic Liquid Crystalline Gels with a Nonuniform Pitch Distribution. *Applied Physics Letters* **2007**, *91*, 201908.

(27) Petriashvili, G.; Japaridze, K.; Devadze, L.; Zurabishvili, C.; Sepashvili, N.; Ponjavidze, N.; Santo, M. P. D.; Matranga, M. A.; Hamdi, R.; Ciuchi, F.; Barberi, R. Paper like Cholesteric Interferential Mirror. *Optics Express* **2013**, *21* (18), 20821.

(28) van Heeswijk E.P.; Meerman T.; de Heer J.; Grossiord N.; Schenning A.P. Paintable encapsulated body-temperature-responsive photonic reflectors with arbitrary shapes. *ACS Applied Polymer Materials*. **2019**; *1*, 3407-12.

(29) Khandelwal, H.; Heeswijk, E. P. A. V.; Schenning, A. P. H. J.; Debije, M. G. Paintable Temperature-Responsive Cholesteric Liquid Crystal Reflectors Encapsulated on a Single Flexible Polymer Substrate. *Journal of Materials Chemistry C* **2019**, *7*, 7395–7398.

(30) Guo, J.; Wu, H.; Chen, F.; Zhang, L.; He, W.; Yang, H.; Wei, J. Fabrication of multi-pitched photonic structure in cholesteric liquid crystals based on a polymer template with helical structure. *Journal of Materials Chemistry* **2010**, *20*, 4094-4102.

(31) Zhang, B.; Lin, X.; You, Y.; Hu, X.; Haan, L. D.; Zhao, W.; Zhou, G.; Yuan, D. Flexible Thermal Responsive Infrared Reflector Based on Cholesteric Liquid Crystals and Polymer Stabilized Cholesteric Liquid Crystals. *Optics Express* **2019**, *27*, 13516.

(32) Khandelwal, H.; Loonen, R. C. G. M.; Hensen, J. L. M.; Debije, M. G.; Schenning, A. P. H. J. Electrically Switchable Polymer Stabilised Broadband Infrared Reflectors and Their Potential as Smart Windows for Energy Saving in Buildings. *Scientific Reports* **2015**, *5*, 11773.

(33) Broer, D. J.; Lub, J.; Mol, G. N. Wide-Band Reflective Polarizers from Cholesteric Polymer Networks with a Pitch Gradient. *Nature* **1995**, *378* (6556), 467–469.

(34) Wang, F.; Li, K.; Song, P.; Wu, X.; Cao, H.; Yang, H. Photoinduced pitch gradients and the reflection behaviour of the broadband films: influence of dye concentration, light intensity, temperature and monomer concentration. *Liquid Crystals*, **2012**, *39*,707-714.

(35) Relaix, S.; Bourgerette, C.; Mitov, M. Broadband reflective cholesteric liquid crystalline gels: volume distribution of reflection properties and polymer network in relation with the geometry of the cell photopolymerization. *Liquid Crystals*, **2007**, *34*,1009-1018.

(36) Bayer, I. S.; Krishnan, K. G.; Robison, R.; Loth, E.; Berry, D. H.; Farrell, T. E.; Crouch, J. D. Thermal Alternating Polymer Nanocomposite (TAPNC) Coating Designed to Prevent Aerodynamic Insect Fouling. *Scientific Reports* **2016**, *6*, 1-13.

(37) Huh, J.-W.; Seo, J.-H.; Oh, S.-W.; Kim, S.-H.; Yoon, T.-H. Tristate Switching of a Liquid-Crystal Cell among Initial Transparent, Haze-Free Dark, and High-Haze Dark States. *Journal of Molecular Liquids* **2019**, *281*, 81–85.

(38) Huh, J.-W.; Yu, B.-H.; Heo, J.; Ji, S.-M.; Yoon, T.-H. Technologies for Display Application of Liquid Crystal Light Shutters. *Molecular Crystals and Liquid Crystals* **2017**, *644*, 120–129.

(39) Huang, Y.; Zhou, Y.; Hong, Q.; Rapaport, A.; Bass, M.; Wu, S.-T. Incident Angle and Polarization Effects on the Dye-Doped Cholesteric Liquid Crystal Laser. *Optics Communications* **2006**, *261*, 91–96.

(40) Tondiglia, V. P.; Rumi, M.; Idehenre, I. U.; Lee, K. M.; Binzer, J. F.; Banerjee, P. P.; Evans, D. R.; Mcconney, M. E.; Bunning, T. J.; White, T. J. Electrical Control of Unpolarized Reflectivity in Polymer-Stabilized Cholesteric Liquid Crystals at Oblique Incidence. *Advanced Optical Materials* **2018**, *6*, 1800957.

(41) Lee, K. M.; Rumi, M.; Mills, M. S.; Reshetnyak, V.; Evans, D. R.; Bunning, T. J.; Mcconney, M. E. A Different Perspective on Cholesteric Liquid Crystals Reveals Unique Color and Polarization Changes. *ACS Applied Materials & Interfaces* **2020**, *12*, 37400–37408.